Viscosity model for the Earth from free oscillations

Igor B. Morozov

Department of Geological Sciences, University of Saskatchewan, Saskatoon, SK S7N 5E2 Canada

SUMMARY

Observations of seismic attenuation within the Earth can be explained in terms of depth variations of viscosity. This allows a description of anelasticity in terms of rigorous mechanical principles without the use of equivalent models or viscoelastic constitutive equations. Compared to the conventional viscoelastic Q, viscosities have a far more general significance in mechanics, are directly measurable and allow straightforward comparisons between different deformations and wave types. "Wet" (Navier-Stokes), "dry" (Coulomb), and other friction regimes are specified by the functional forms of Lagrangian dissipation functions. All creep phenomena and attenuation of traveling and standing waves are consistently described in the viscosity model. The characteristic rock viscosity in laboratory creep experiments is estimated as $\sim 10^{14}$ Pa·s.

The model is illustrated on the whole-Earth free-oscillation Q dataset by Widmer *et al*. (*Geophys. J. Int*., 104, 541–553, 1991). When transformed into temporal attenuation coefficients, $\chi = \pi f Q^{-1}$, the data reveal near-linear trends with frequency, $\chi \propto \omega$, for fundamental modes, and quadratic trends $\chi \propto \omega^2$ for radial modes. Similar relations $\chi \propto \omega^2$ are also found for PKIKP body waves within the inner core. This shows that energy dissipation is mostly "dry" within the mantle and more "wet" within the core. Inversion suggests pronounced layering of viscosity within the Earth, and particularly within its lower mantle. Seismic viscosity is $\sim 30 \cdot 10^{10}$ Pa·s within the mantle lid, $\sim 6–10 \cdot 10^{10}$ Pa·s within the upper mantle, and 6 to $20 \cdot 10^{10}$ Pa·s within the lower-mantle layers. Broadly, this is similar to the existing Q models, although a quantitative comparison is difficult because of the frequency dependencies built into the viscoelastic model. The layering of mantle viscosity is also similar to that in geodynamic models. Within the outer core, the viscosity is near zero, and the inner-core viscosity is $\sim 0.5–1 \cdot 10^{10}$ Pa·s. Thus, by contrast to the existing Q models, the attenuation within the inner core is found to be much weaker than within the mantle.

Introduction

Analysis of energy dissipation at the global scale is most important for understanding the temperature and physical state of the Earth's interior. Several depth profiles of the quality factor Q have been developed, which are generally close to the reference model PREM (Dziewonski and Anderson, 1981), and extensive development of 3D tomographic models is underway (Romanowicz and Mitchell, 2009). The analysis of anelasticity is complicated by the difficulties of accurate measurement of Q, which is often affected by noise and the effects of structure, such as normal-mode splitting and beating or variations of geometrical spreading. Since the observed quality factors usually exceed ~100, anelasticity represents a relatively small effect compared to the geometrical and elastic factors, and its measurements are accordingly delicate. Some difficulties arise from the discrepancies between the surface-wave and normal-mode attenuation measurements at 200–500-s periods (Durek and Ekström, 1997).

However, in addition to the observational difficulty, there also exists another, conceptual problem in analysing the global anelastic structure: the concept of Q as an *in situ* parameter of the medium may be inadequate for describing the anelasticity of the Earth. This fundamental problem has received no attention so far, and yet its effect can be much greater than the observational uncertainties. Looking back at the history of the seismic Q, one can see that it was inferred from analogies with mechanical oscillators or electrical circuit theory (*e.g.*, Knopoff and MacDonald, 1958). However, if taken to the level of local medium properties, such analogies may become imprecise or misplaced. The mechanical or electrical "quality" Q is a parameter of a resonator, equal to the ratio of its natural frequency to the spectral bandwidth; by contrast, a wave-propagating medium shows no resonance peaks.

The existing models of anelasticity are formulated in terms of the bulk and shear quality factors Q_K and Q_μ, which are associated with the corresponding elastic moduli K and μ (Dziewonski and Anderson, 1981; Widmer *et al.*, 1991; Dahlen & Tromp, 1998; Romanowicz & Mitchell, 2009). This two-parameter description is formalized in the viscoelastic model, in which the dissipation of elastic energy is explained by some "imperfect" behaviour of the elastic moduli, which is mathematically expressed by phase delays shifts in the strain-stress relations (Anderson & Archambeau, 1964). Such treatment of anelasticity as extrapolation of the elastic case into the complex planes of elastic parameters is also known as the correspondence principle (Aki & Richards, 2002). Although the pair of viscoelastic parameters is sufficient for reproducing most of the available observations of seismic-wave attenuation, this description is nevertheless unsatisfactory. Physically, it is difficult to agree that dissipation of elastic energy would occur in different but fixed proportions of the bulk and shear energies and at the same time be unrelated to the kinetic energy. As discussed below, in mechanics, the situation is the opposite. Seismic viscoelasticity may be the only theory in which the observable attribute (Q) is also viewed as an intrinsic property of the medium. Instead of being derived from real physical properties, the *in situ* Q^{-1} is basically defined as such a quantity which reproduces the observed Q^{-1} when treated as complex argument of the wave speed. This leads to a mathematical model which describes the selected group of observations but may not extend to the more general cases. Note that seismic viscoelasticity contains no rigorous definition of elastic energy (*e.g.*, Carcione, 2007), which makes it questionable with respect to predicting energy balance and dissipation.

From the viewpoint of elastic-continuum mechanics, energy dissipation does not have to be "viscoelastic." Successful physical models of attenuative media (*e.g.*, Biot, 1956; Deresiewicz, 1960; Beskos *et al.*, 1989) are neither based on nor lead to the concept of a "medium Q." Instead, such models reveal numerous properties (such as porosity, permeability, fluid content, viscosity) that are responsible for the dissipation of elastic-wave energy. Most of these properties are

unrelated to the elastic moduli and require specific mechanisms and descriptions.

Along with the use of only two *in situ* parameters Q_K and Q_μ, serious practical limitations also arise from the viscoelastic model of seismic attenuation. For example, in this model, the rate of shear-energy dissipation equals μQ_μ^{-1}, which is proportional to μ. Therefore, the shear-wave part of energy dissipation within the liquid outer core is automatically zero, and consequently its Q_μ^{-1} is also set equal zero in all existing models (*e.g.*, Dziewonski & Anderson, 1981; Widmer *et al.*, 1991). However, such *a priori* absence of energy dissipation within the outer core appears unnatural, as shear deformations within this region are significant for many free-oscillation modes, and it should also possess some viscosity. In additional illustrations, the correspondence principle leads to incorrect phases of the acoustic impedance in anelastic heterogeneous media (Morozov, 2011) and to 10–20% over-estimations of dissipation for mantle Love waves (Morozov, submitted to *PEPI*).

Thus, it appears worthwhile to try an alternate characterization of the whole-Earth's attenuation, which would be based on the traditional mechanics rather than on viscoelastic postulates. As shown below, such formulation can be based on the concept of macroscopic viscosity of the Earth. This quantity has a tangible physical meaning, and unlike the *in situ Q*, it can in principle be measured in other than *Q*-type experiments. An interpretation in terms of physical properties should also help reconciling the free-oscillation attenuation models with those derived from ScS and core body-wave datasets (Bhattacharyya *et al.*, 1996; Cormier & Li, 2002; Li & Cormier, 2002; Lawrence & Wysession, 2006). However, changing the viewpoint so dramatically still does not mean that the existing attenuation models presented in terms of *Q* become completely wrong or irrelevant. Several features of the existing *Q* distributions are also present in viscosity models discussed below. At the same time, switching to a more "physical" picture shows that some of the assumptions intended as simplifying (such as a frequency-independent or smoothly-varying *Q*) may in fact be unjustified and even lead to some confusion. The question of frequency dependence of *Q* (*e.g.*, Lekić, *et al.*, 2009; Morozov, 2010a) also disappears and is superseded by the more general problem of the physical mechanisms of anelasticity.

Unfortunately, it is already clear that a realistic "physical" theory of the Earth should be significantly more complex than the viscoelastic model, and even the key principles of such a theory are unclear at present. Early researchers (*e.g.*, Knopoff & MacDonald, 1958) attempted strictly mechanical descriptions but were apparently discouraged by the difficulties of explaining the frequency-independent *Q*, which was the predominant observation at the time. Since then, this argument has lost its power, as it is now commonly known that *Q* varies with frequency. Nevertheless, mechanical models of attenuation seem to have been nearly forgotten in global seismology.

In this paper, we try reviving the mechanical approach by using a simple Lagrangian formulation close to the model of saturated porous rock by Biot (1956). The key principle of this approach is in describing the dynamic properties of the medium *before* any equations of motion are formulated. This is the most important requirement to consistent physical theories (Landau & Lifshitz, 1976), which is also not satisfied by the viscoelasticity. Instead of the *in situ Q*, we describe the energy dissipation by bulk, shear, and kinetic viscosity parameters, denoted η_Δ, η_ε and η_k below. Although still phenomenological (macroscopic) in character, these parameters have clear physical meanings, act "instantaneously" and are local within the structure, which cannot be said about the "medium *Q*" (cf. Morozov, 2009). Although bearing some mathematical similarities to K, μ and ρ, these viscosity parameters may (or may not) be totally unrelated to the elastic moduli. Once the physical mechanisms of energy dissipation within the Earth become better understood, this model can be further developed by adding other parameters and functional

forms.

The free-oscillation problem represents a good case to study the fundamental physics of Earth's attenuation. Normal modes behave as mechanical oscillators, for which the quality factor is meaningful and the physical theory is developed in detail. Free oscillations are sensitive to all three elastic parameters of the Earth, and they provide the critical constraints for global elastic and anelastic models (Dziewonski & Anderson, 1981). The free-oscillation problem is also where the Lagrangian mechanics is recognised and used by seismologists (Woodhouse and Deuss, 2009). The whole-Earth environment also offers a broad range of variations in mechanical parameters, which allows studying their effects on the observed frequencies and quality factors of normal modes. At the same time, the general methodology of the present study naturally extends to many other areas of elastic-wave attenuation analysis. In the following sections, we introduce this basic methodology, discuss its relation to the existing theory of and the key effects of seismic attenuation, and finally apply to the inversion of normal-mode *Q*.

Approach

We will use the Lagrangian formalism for describing the mechanics of an elastic medium. This description starts with the Lagrangian density, which is a quadratic functional of the displacements u_i and velocities $\dot{u}_i$:

$$L\left\{\mathbf{u},\dot{\mathbf{u}}\right\} = \frac{\rho}{2}\dot{u}_i\,\dot{u}_i - \frac{\lambda}{2}\varepsilon_{kk}\varepsilon_{ll} - \mu\varepsilon_{ij}\varepsilon_{ij}\,, \tag{1}$$

where i = 1, 2, or 3 denotes the spatial dimensions, $\varepsilon_{ij} = \left(\partial_i u_j + \partial_j u_i\right)\big/2$ is the strain tensor, and summations over all pairs of repeated indices are assumed. Parameters λ and μ are the Lamé elastic constants, and ρ is the mass density. Note that both the displacements and velocities are viewed as independent variables in the functional (1). Most importantly, coefficients ρ, λ and μ are real-valued and non-negative, which makes expression (1) real and positive-definite with respect to all variables. This is already the first and most important difference of this model from viscoelasticity.

By replacing ε_{ij} with a combination of the dilatational strain $\Delta = \varepsilon_{kk}$ and deviatoric strain $\tilde{\varepsilon}_{ij} = \varepsilon_{ij} - \Delta\delta_{ij}\big/3$, the Lagrangian density becomes expressed in terms of the bulk (K) and shear (μ) moduli:

$$L = \frac{\rho}{2}\dot{u}_i\,\dot{u}_i - \frac{K}{2}\Delta^2 - \mu\tilde{\varepsilon}_{ij}\tilde{\varepsilon}_{ij}\,. \tag{2}$$

Energy dissipation is not a part of the Lagrangian and is described by the dissipation function D (Landau & Lifshitz, 1976). In the small-amplitude approximation, if we assume a linear viscous friction force proportional to $\dot{u}_i$, D should be second-order in $\dot{u}_i$. For an instructive mechanical analog, let us consider the linear oscillator. Its Lagrangian is

$$L\left(x,\dot{x}\right) = E_k - E_p \equiv \frac{m}{2}\dot{x}^2 - \frac{m\omega_0^2}{2}x^2\,, \tag{3}$$

and dissipation function:

$$D_{visc} = \eta \frac{m}{2} \dot{x}^2 = \xi \omega_0 E_k , \tag{4}$$

where E_k and E_p are the kinetic and potential energies, respectively, m is the mass, ω_0 is the natural frequency, η is the viscosity, and $\xi = \eta/m\omega_0$ is the dimensionless dissipation constant. This dissipation function corresponds to a linear viscous force of $f_D \equiv \partial D / \partial \dot{x} = -\eta \dot{x}$ and has the physical meaning of energy dissipation rate per unit time. Note that function D for the oscillator equals its kinetic energy divided by "relaxation time" $\tau_0 = 1/(\xi\omega_0) = m/\eta$. Mean total energy of the oscillator decays with time as:

$$\frac{\left\langle E_{total}(t) \right\rangle}{E_0} = \exp\left(-\frac{t}{\tau_0} \right), \tag{5}$$

where E_0 is the total energy at $t = 0$. If we now consider a Coulomb ("dry") force of friction σ_D, which is independent of velocity: $f_D = -\sigma_D \operatorname{sgn}(\dot{x})$, the dissipation function (4) is replaced with

$$D_{dry} = \sigma_D |\dot{x}| = \sigma_D \sqrt{\frac{2}{m}} E_k^{1/2} , \tag{6}$$

i.e. it becomes proportional to a square root of the kinetic energy. In this case, the mean energy decay law (5) is non-exponential, but it can be approximated as such for relatively short times:

$$\frac{\left\langle E_{total}(t) \right\rangle}{E_0} = \left(1 - \frac{6\sigma_D}{\sqrt{mE_0^3}} t \right)^{2/3} \approx \exp\left(-\frac{t}{\tau_0} \right), \tag{7}$$

where $\tau_0 = \sqrt{mE_0^3} / (4\sigma_D)$. In all cases, the quality factor of the oscillator simply represents the ratio of the energy decay time τ_0 to the period of oscillation, T_0:

$$Q = \tau_0 \omega_0 = 2\pi \frac{\tau_0}{T_0} . \tag{8}$$

Note that Q is a property of the entire oscillator and not of any of its elastic constant or mass. The often-discussed "frequency dependence if Q" thus represents a scaling problem rather than a fundamental property of the material (Morozov, 2010a, b). If we scale the frequency of the oscillator by increasing its elastic constant $k = m\omega_0^2$, then Q increases proportionally to ω_0. Conversely, if we increase ω_0 by decreasing m, Q decreases as ω_0^{-1}. We can also increase k and decrease m proportionally to $\sqrt{\omega_0}$, which will keep Q constant. Apart from this (somewhat confusing) scaling, Q^{-1} is actually proportional to the friction constants η in (4) or σ_D in (6).

In constructing a functional D similar to (4) and (6), and also in defining a Q similar to (8) for the Earth's medium, there exists a fundamental difficulty, which is the absence of an analog to the natural frequency ω_0. Traveling waves represent purely forced oscillations, and

although there exist natural analogs to η and τ_0, quantities ω_0 and ξ above can hardly be defined as medium attributes (Morozov, 2009). For guidance in describing the elastic-energy dissipation within the medium, we can use Biot's (1956) model of saturated porous rock. In this model, energy dissipation is caused by relative movement of the pore fluid with respect to the rock matrix. This movement is described by the filtration velocity, $\dot{\mathbf{w}} = \dot{\mathbf{U}} - \dot{\mathbf{u}}$, where $\dot{\mathbf{U}}$ and $\dot{\mathbf{u}}$ are the fluid and matrix velocities, respectively. The dissipation-function density is defined as the only rotationally-invariant scalar which is quadratic in $\dot{\mathbf{w}}$:

$$D = \frac{\eta}{2\kappa} \dot{w}_i \dot{w}_i . \tag{9}$$

Here, η is the fluid viscosity, and κ is the absolute permeability, which depends on the geometry of the pores and other factors. The Lagrangian density (1) is also modified by the presence of pore fluid, into which we will not go at the moment. A good summary of Biot's theory is given by Bourbié *et al*. (1987).

Because at this stage we have no justification for a multiphase model of the mantle which would contain internal variables similar to $\dot{\mathbf{w}}$ above, we construct the dissipation function by a heuristic generalization of expressions (2), (4), and (6). When using only $\dot{u}_i$ for parameterizing the flow in an isotropic medium, the only three rotationally-invariant second-order scalar functions are $\dot{u}_i \dot{u}_i$, $\dot{\Delta}^2$ and $\dot{\tilde{\varepsilon}}_{ij} \dot{\tilde{\varepsilon}}_{ij}$. Therefore, we define a generalized dissipation function by combining these invariants:

$$D = \frac{\eta_k \rho_0}{2K_0} \dot{u}_i \dot{u}_i + \frac{\eta_\Delta}{2} \dot{\Delta}^2 + \eta_\varepsilon \dot{\tilde{\varepsilon}}_{ij} \dot{\tilde{\varepsilon}}_{ij} . \tag{10}$$

Here, η_Δ and η_ε are the bulk and shear viscosities known in Navier-Stokes equations in fluid mechanics (Landau & Lifshitz, 1987). These terms were briefly considered in the "hypothetical" anelasticity model in Morozov (2010c). The term with η_ε in (10) also corresponds to a Kelvin-Voigt solid, and Jeffreys characterized such behaviour as "firmoviscous" (see Knopoff and MacDonald, 1958). For fluids, parameter η_ε is usually called simply *viscosity*, or *dynamic viscosity*, and η_Δ is called *second viscosity* and often disregarded for incompressible fluids. The "kinetic viscosity" term η_k here is added for completeness. Because this term depends on the velocities $\dot{u}_i$ and not on their gradients, it may violate the Galilean principle of relativity and should be taken with some caution. However, this principle may not be required in the whole-Earth problem, in which there exists a preferred frame of reference. In the examples below, η_k is not considered, but it was used in the surface-wave model by Morozov (submitted). Reference elastic module K_0 and density factor ρ_0 are included in (10) in order to ensure the same units [Pa·s] for η_k, η_Δ and η_ε, and they play the role of the absolute permeability factor κ in (9).

To clarify the terminology, note that the model defined by expressions (2) and (10) is truly "visco-elastic," in the sense of combining the viscous and elastic properties of the medium. However, historically, the term "viscoelastic" has been firmly linked to a specific model addressing the same general question by using time-retarded constitutive equations, equivalent dashpot-spring models, and complex wave speeds (Cormier, 2011). In this paper, we also retain such specific meaning of this term.

To explore a non-linear energy dissipation similar to eq. (6), we can introduce exponents

ν_Δ, ν_ε and ν_k into (10) to accommodate the transitions from the viscous-flow ($\nu = 1$, similarly to eq. (4)) to dry-friction regimes ($\nu = 1/2$, as in eq. (6)):

$$D = \frac{1}{\tau_r^2}\left[\frac{\eta_k \rho_0}{K_0}\left(\frac{\dot{u}_i \dot{u}_i}{2}\tau_r^2\right)^{\nu_k} + \eta_\Delta\left(\frac{\dot{\Delta}^2}{2}\tau_r^2\right)^{\nu_\Delta} + \eta_\varepsilon\left(\dot{\tilde{\varepsilon}}_{ij}\dot{\tilde{\varepsilon}}_{ij}\tau_r^2\right)^{\nu_\varepsilon}\right]. \tag{11}$$

This shows that non-linearity also leads to a characteristic time scale, τ_r, which is required in order to maintain the correct dimensionality of D. With varying τ_r, η_Δ, η_ε and η_k would scale accordingly. Because of this scaling ambiguity and without loss of generality, parameter τ_r can therefore be set by convention, for example, equal 1 s.

Viscosity parameters η_Δ, η_ε and η_k represent the *in situ* physical variables of our model and can be viewed as extensions of the heuristic "intrinsic attenuation coefficient" of the medium proposed by Morozov (2010b). To form the system of equations to invert for these parameters, we need to express the observed attenuation coefficient for any given wave mode n:

$$\chi_n = \frac{\langle D\rangle_n}{\langle E_{total}\rangle_n} = \frac{1}{\tau_r^2\langle E_{total}\rangle_n}\left[\frac{\eta_k\rho_0}{K_0}\left\langle\left(\frac{\dot{u}_i\dot{u}_i}{2}\tau_r^2\right)^{\nu_k}\right\rangle_n + \eta_\Delta\left\langle\left(\frac{\dot{\Delta}^2}{2}\tau_r^2\right)^{\nu_\Delta}\right\rangle_n + \eta_\varepsilon\left\langle\left(\dot{\tilde{\varepsilon}}_{ij}\dot{\tilde{\varepsilon}}_{ij}\tau_r^2\right)^{\nu_\varepsilon}\right\rangle_n\right], \tag{12}$$

where $\langle ... \rangle_n$ denotes an integration over the entire space, and E_{total} is the total energy density. Note that for both traveling and standing harmonic waves with low dissipation, the total energy is equipartitioned (Dahlen & Tromp, 1998):

$$\langle E_{kinetic}\rangle_n = \langle E_{potential}\rangle_n = \frac{1}{2}\langle E_{total}\rangle_n, \tag{13}$$

In the approximation considered here, the forward problem (12) is linear in η_Δ, η_ε and η_k.

Creep, Q, and dispersion

The linear viscosity model (10) readily explains all of the observable effects of seismic anelasticity, such as creep, wave attenuation and dispersion. This model can even be used to infer the viscoelastic bulk and shear quality factors of the medium. Let us illustrate these properties on a simple case of unidirectional deformation.

For a deformation in the direction of axis X, $\mathbf{u} = (u,0,0)$, and the Lagrangian density (2) simplifies to:

$$L = \frac{\rho}{2}\dot{u}^2 - \frac{M}{2}\left(\partial_x u\right)^2, \tag{14}$$

where $M = K + \frac{4}{3}\mu$ is the P-wave modulus. Similarly, the dissipation density (10) is:

$$D = \frac{\eta_k\rho_0}{2K_0}\dot{u}^2 + \frac{\eta_M}{2}\left(\partial_x\dot{u}\right)^2, \tag{15}$$

where $\eta_M = \eta_\Delta + \frac{4}{3}\eta_\varepsilon$.

To derive the equation of creep, consider a quasi-static deformation, under which a body of thickness H is uniformly extended by strain factor $\varepsilon(t)$: $u(x,t) = x\varepsilon(t)$, where $0 \le x \le H$. Let us assume that this deformation is achieved by an external force f applied at point $x = H$. Taking for simplicity $\eta_k = 0$ and considering only linear dissipation ($\nu = 1$), the total Lagrangian and the dissipation function from (14) and (15) become:

$$\mathbb{L} = \int_0^H L dx + fH\varepsilon = \frac{\rho H^3}{6}\dot{\varepsilon}^2 - \frac{MH}{2}\varepsilon^2 + fH\varepsilon \text{, and } \mathbb{D} = \int_0^H D dx = \frac{\eta_M H}{2}\dot{\varepsilon}^2 \ . \tag{16}$$

The Euler-Lagrange equation of motion is therefore:

$$\frac{d}{dt}\left(\frac{\delta \mathbb{L}}{\delta \dot{\varepsilon}}\right) - \frac{\delta \mathbb{L}}{\delta \varepsilon} + \frac{\delta \mathbb{D}}{\delta \dot{\varepsilon}} = \frac{\rho H^3}{3}\ddot{\varepsilon} + MH\varepsilon + \eta_M H\dot{\varepsilon} - fH = 0 \, . \tag{17}$$

The corresponding homogenous equation (with $f = 0$) has two exponential solutions:

$$\varepsilon_{1,2}(t) = A_{1,2}\exp\left(-\frac{t}{\tau_{1,2}}\right) , \tag{18}$$

where $\tau_{1,2}$ are the relaxation times:

$$\tau_{1,2} = \frac{2\rho H^2}{3\eta_M}\left(1 \pm \sqrt{1 - \frac{4\rho H^2 M}{3\eta_M^2}}\right)^{-1} . \tag{19}$$

For $\eta_M^2 >> 4\rho H^2 M/3$, these relaxation times equal $\tau_1 \approx \frac{\rho H^2}{3\eta_M}$ and $\tau_2 \approx \frac{\eta_M}{M}$, and consequently $\tau_1 << \tau_2$. Thus, over some initial time interval, the system quickly equilibrates, after which it continues to "creep" slowly (Figure 1). In the process of equilibration, other "normal modes" need to be considered in addition to the uniform deformation above, such as $u_n(x,t) = \sin\left(\frac{\pi n}{2H}x\right)\varepsilon_n(t)$ with $n = 1,2,3,...$ However, these initial oscillations should decay within several natural oscillations of the specimen:

$$T_n = \frac{2H}{n}\sqrt{\frac{\rho}{M}} \, . \tag{20}$$

For typical laboratory specimen sizes, $\tau_1 << T_1$, and therefore T_1 can be taken as the characteristic equilibration time. The total deformation ε_U at $t >> T_1$ is therefore:

$$\varepsilon(t) = \varepsilon_U + (\varepsilon_R - \varepsilon_U)\left[1 - \exp\left(-\frac{t}{\tau_2}\right)\right], \tag{21}$$

where $\varepsilon_R = f/M$ is the static, "relaxed" deformation at $t \to \infty$, and ε_U is the "unrelaxed" deformation after the equilibration, at $T_1 << t << \tau_2$. This quantity can be derived by setting the inertial term containing $\ddot{\varepsilon}$ equal zero in eq. (17):

$$\varepsilon_U = \varepsilon_R - \frac{f\tau_2^2}{\eta_M \tau_2 - \frac{\rho H^2}{3}}. \tag{22}$$

From the above relations, taking typical values of $\tau_2 \approx 10^3$ s and $M \approx 10^{11}$ Pa in a laboratory creep experiment, we can estimate rock viscosity as $\eta_M \approx 10^{14}$ Pa·s. For a rock sample of $H \approx 0.1$ m size, the equilibration times are then $\tau_1 \approx 10^{-13}$ s and $T_1 \approx 10^{-5}$ s. The inverse of T_1, $a = T_1^{-1} \approx 10^5$ Hz, could correspond to the characteristic frequency a in the empirical creep law by Lomnitz (1956).

As we see, the model (10) naturally describes creep phenomena (Figure 1) without assuming phase-delayed strain-stress relations. Obviously, this example can be continued by constructing the creep function, equivalent models, frequency-dependent Q, absorption band, and all other attributes of viscoelastic constitutive relations.

For another important example, let us now consider plane waves traveling within a uniform attenuating medium. Such waves decay exponentially, and the corresponding Q factors can be inferred from their spatial attenuation coefficients. By contrast to the case of creep, we now deal with weak energy dissipation: $\omega\eta_M << M$, where ω is the angular frequency. For a harmonic P wave, $u(x,t) = \bar{u}(x)\exp(-i\omega t)$, and eqs. (14) and (15) lead to the spatial (Helmholtz) equation of motion:

$$\frac{\delta L}{\delta u} - \frac{\delta D}{\delta \dot{u}} = \left(\omega^2\rho + i\omega\frac{\eta_k\rho_0}{2K_0}\right)\bar{u} - \left[M - i\omega\eta_M\right]\partial_x^2\bar{u} = 0. \tag{23}$$

Again considering $\eta_k = 0$, we obtain the complex wavenumber:

$$k_P = \omega\sqrt{\frac{\rho}{M - i\omega\eta_M}} \approx \omega\sqrt{\frac{\rho}{M}}\left(1 + \frac{i\omega\eta_M}{2M}\right). \tag{24}$$

The "specific attenuation factor" (Knopoff and MacDonald, 1958) for P wave is therefore:

$$Q_P^{-1} = 2\arg k_P \approx \omega\frac{\eta_M}{M}. \tag{25}$$

as expected in a Kelvin-Voigt solid. Note that it turns out that $Q_P^{-1} = \omega\tau_2$, where τ_2 is the creep relaxation time (19) (Figure 1). Similarly, for an S wave, Q_S^{-1} equals:

$$Q_S^{-1} = 2\arg k_S \approx \omega\frac{\eta_\varepsilon}{\mu}. \tag{26}$$

Formula (24) also shows that viscosity leads to weak phase-velocity dispersion:

$$V_P(\omega) = \frac{\omega}{\mathrm{Re}\,k} \approx \omega\sqrt{\frac{\rho}{M}}\left[1 - \frac{7}{8}\left(\frac{\omega\eta_M}{M}\right)^2\right]. \tag{27}$$

It should be noted that as all of the above results, this equation only describes the plane-wave dispersion in a uniform medium. In more general cases, dispersion is principally controlled by the propagating structures, such as layering for surface waves and normal modes. Once again, we have to disagree with the popular notion of "physical dispersion" as a $V(\omega)$ variation resulting purely from anelasticity (Kanamori & Anderson, 1977). Simple phase-velocity relations like

$$V(\omega) = V(\omega_r)\left[1 + \frac{1}{\pi Q}\ln\left(\frac{\omega}{\omega_r}\right)\right], \tag{28}$$

or the corresponding relations inferred for the moduli, such as (Dahlen & Tromp, 1998):

$$\mu(\omega) = \mu(\omega_r)\left[1 + \frac{2}{\pi Q}\ln\left(\frac{\omega}{\omega_r}\right)\right], \tag{29}$$

indeed arise, but *only in viscoelastic models*, in which Q is *the only* medium parameter responsible for any deviations from the elastic case and in which one can take $\mu = \rho V^2$. In reality, multiple factors influence the attenuation and dispersion, and both $Q(\omega)$ and $V(\omega)$ are determined largely *independently* by complex combinations of these factors. Expression (28) is usually derived from the Kramers-Krönig causality relations (Kanamori & Anderson, 1977; Aki & Richards, 2002); however, these relations only represent integral identities satisfied by the resulting *wave solutions*. These identities do not directly constrain any properties of the propagating medium. Any wave in the medium described by eqs. (2), (10), and (11) would be causal and automatically satisfy the Kramers-Krönig relations.

From the above plane-wave Q's, values of Q_K^{-1} and Q_μ^{-1} can be further inferred by using the following postulates of seismic viscoelasticity (Anderson & Archambeau, 1964): 1) both phase velocities, $c_{P,S} = \omega/k_{P,S}$, equal the P and S-wave speeds, $V_P = \sqrt{M/\rho}$ and $V_S = \sqrt{\mu/\rho}$, respectively, 2) V_P, V_S, and the viscoelastic moduli M and μ become complex-valued, with $(-Q^{-1})$ interpreted as their complex arguments, and 3) density ρ remains real. From these assumptions, $Q_M^{-1} = Q_P^{-1}$ and $Q_\mu^{-1} = Q_S^{-1}$. The bulk viscoelastic attenuation is then:

$$Q_K^{-1} \equiv -\arg\tilde{K} \approx \frac{MQ_P^{-1} - \frac{4}{3}\mu Q_S^{-1}}{K}, \tag{30}$$

where the complex moduli are related by $\tilde{K} = \tilde{M} - \frac{4}{3}\tilde{\mu}$. Taking into account expressions (25) and (26), this gives:

$$Q_K^{-1} \approx \omega \frac{\eta_M - \frac{4}{3}\eta_\mu}{K} = \omega \frac{\eta_\Delta}{K}. \qquad (31)$$

Thus, the linear model (10) leads to spatial attenuation coefficients Imk_P and Imk_S proportional to ω^2 (see eq. (24)), and accordingly, Q_P and Q_S are proportional toω^{-1}. Such behaviour commonly arises in mechanical systems with weak linear dissipation (Knopoff & MacDonald, 1958), including Biot's (1956) model of saturated porous rock. Similar ω^{-1} dependencies also follow for Q_K and Q_μ (eqs. (31) and (26)). However, note that as the above derivation shows, these quantities are quite artificial and only remotely related to the corresponding elastic moduli. Their principal meaning still remains as the transformed Q_P and Q_S values, which in their turn, only arise in special cases of plane or spherical waves in a uniform isotropic medium.

Existing whole-Earth models from free oscillations

Two well-known spherically-symmetric models of Earth's seismic anelasticity: PREM (Dziewonski & Anderson, 1981) and QM1 (Widmer *et al*., 1991), are shown in Figure 2. Both models were developed within the viscoelastic paradigm and parameterized by frequency-independent Q_K^{-1} and Q_μ^{-1} (Figure 2a). By using eqs. (25) and (31), we also transformed them into the corresponding bulk and shear viscosities (Figure 2b).

The above transformation from Q^{-1} to viscosity highlights several issues inherent in the existing parameterization of Earth's attenuation. First, it is often noted that the upper mantle is the region of the highest attenuation within the mantle (*e.g*., Anderson & Archambeau, 1964; Widmer *et al*., 1991; Durek & Ekström, 1996; Romanowicz & Mitchell, 2009). However, this is only true if the term "attenuation" is understood as the value of Q^{-1} (Figure 2a). If we interpret the attenuation in the more intuitive (or physical) sense, as the relative energy dissipation per second, then the lower one third of the mantle turns out to be more attenuative than the upper mantle (Figure 2b). The attenuation within the inner core also becomes ~2 times greater than within the upper mantle.

Second, it is generally known that the frequency dependence of Q is difficult to constrain from normal-mode or surface-wave data (Widmer *et al*., 1991; Durek & Ekström, 1996), although some authors argue the contrary (Lekić *et al*., 2009). In consequence, many models use what appears to be the simplest parameterization, which is the frequency-independent Q. However, this leads to viscosities decreasing with frequency (Figure 2b), which may not be easy to understand. As our mechanical argument above suggests, a "natural" frequency dependence of the *in situ* Q corresponding to constant viscosity would be somewhere between $Q \propto \omega^{-1}$to ω^0. Unfortunately, such frequency dependencies are not commonly considered in attenuation studies.

The third serious issue with the models shown in Figure 2b is the built-in correlation of their viscosity parameters with the elastic moduli. This leads to preferentially positive depth gradients in η_μ and the amount of detail that can hardly be constrained from attenuation data. In particular, this results in a virtual disappearance of attenuation across the core-mantle and inner-core boundaries because of the zero shear modulus of the outer core (Figure 2b). Note that in the existing Q models, such zero shear attenuation within the outer core is dictated not by the data but purely by an abstract methodological (*i.e*., correspondence) principle. However, this principle is only inferred from simple uniform-medium cases and may not apply to the heterogeneous Earth (Morozov, 2011).

Nevertheless, with the above uncertainties, the ranges and general pattern of viscosity

variations shown in Figure 2b should be correct. This will be illustrated by a new inversion performed in the following section. As expected, these viscosities are much lower than those inferred from geodynamic studies (~$5 \cdot 10^{20}$ Pa·s within the upper and 10^{18}–10^{24} Pa·s within the lower mantle; also see *Discussion* below), but are within the range of values estimated for the outer core (10^{3}–10^{11} Pa·s; S. Butler, personal communication).

New model of normal-mode attenuation

Dataset

To measure the seismic viscosity parameters of the Earth, we use a free-oscillation dataset compiled by Widmer *et al*. (1991). For details of data selection and measurements of the modal frequencies and Q, the reader is referred to that paper. Although new and corrected normal-mode data have been acquired since its publication, the dataset is still significant in size (116 spheroidal and 30 toroidal modes), carefully checked, and well presented. Compiling normal-mode frequency and Q data is a very substantial and intricate effort in itself (*e.g.*, Laske & Widmer-Schnidrig, 2009), and our objective here is only to look at a well-established dataset from a new physical standpoint. In this way, we can also directly compare our results to the previous inversions, three versions of which were shown by Widmer *et al*., (1991).

In order to produce the forward kernels, similarly to Widmer *et al*. (1991), we used the Mineos package currently distributed under an open-source license by the Computational Infrastructure for Geodynamics (http://geodynamics.org/cig/). This code has a long history of development, starting from J. F. Gilbert in about 1966 and major enhancements by J. Woodhouse in 1980, followed by many improvements and maintenance by G. Masters, M. Ritzwoller, and M. Barmine since then. We only used the main Mineos program for computing the normal-mode frequencies and eigenfunctions, which were further rescaled according to the normalization convention of Dahlen & Tromp (1998) and checked for energy equipartitioning. We used the elastic part of PREM model without oceans, which was different from the study by Widmer *et al*. (1991), who used an earlier elastic model 1066A (Gilbert & Dziewonski, 1975). Nevertheless, as Widmer *et al*. (1991) noted, the selected modes should not be very sensitive to the detail of the elastic structure. Further processing of the eigenfunctions, including interfacing with Octave for inversion, was performed by the "well-log" part of our IGeoS package (Morozov, 2008a; Morozov & Pavlis, 2011).

The spherical-Earth eigenfunctions U, V, and W (Dahlen & Tromp, 1998) corresponding to four groups of selected modes are shown in Figure 3. Note that each group has a characteristic general pattern of amplitude variations with depth. In particular, radial modes are relatively uniformly distributed in depth (Figure 3a), and the energy distributions within the fundamental modes ${}_nS_0$ progressively shift toward the surface with increasing radial numbers n, which also correspond to increasing oscillation frequencies (Figures 3b, d, and e).

Direct observations from the data

Some constraints on the resulting models (10), (11) can be derived directly from the observed attenuation data (Figure 4). Conventionally, such data are shown in the form of $q = 1000Q^{-1}$, which is cross-plotted against modal frequencies in Figures 4b and d. However, as demonstrated on a number of datasets (Morozov, 2008b, 2010a, b), reverse transformation of such Q^{-1} data into the temporal attenuation coefficient, $\chi = \pi f Q^{-1}$, often reveals data trends that are simpler and often remain unnoticed in the form of a frequency-dependent Q^{-1}. Such (f, χ) cross-plots for the data of this study are shown in Figures 4a and c. Note that in normal-mode observations, χ represents an estimate for the modal peak in the amplitude spectrum, which is

measured directly and from which the Q^{-1} is inferred. In theoretical modeling, χ also represents the primary variable, which is the imaginary part of complex frequency. Therefore, the entire modeling, inversion, and interpretation can be conducted in the form of χ, and similarly to the *in situ Q*, the use of modal *Q* is not required.

In the generalized model (11), because of the time derivatives, the characteristic frequency dependence of each term is $\chi_i \propto \omega^{2\nu_{k,\Delta,\varepsilon}}$. Because each of these terms must be non-negative, this would lead to the corresponding increase in the observed $d\chi/d\omega$ with frequency. On the other hand, the observed attenuation coefficients for spheroidal modes (grey dotted lines in Figure 4a) show near-linear trends at $f_0 < 2.5$ mHz and $f_0 > 3.5$ mHz, similar to the empirical linear $\chi(f)$ trends suggested from many datasets by Morozov (2008b, 2010a–c). Radial and fundamental spheroidal modes with $f_0 > 2.5$ mHz are close to the quadratic trends $\chi \propto \omega^2$ or $Q^{-1} \propto \omega$ (dashed lines in Figures 4a and b). The fundamental toroidal modes (Figure 4c) are inconsistent with a $\chi \propto \omega^2$ trend and strongly suggest a near-linear dependence.

The empirical observations above suggest that exponents ν_k, ν_Δ, and ν_ε in (11) should be variable with depth. In the iterative inversion process described in the following section, we therefore selected $\nu_\varepsilon = 1$ within the core and $\nu_\varepsilon = 0.6$ within the mantle. Thus, the observed quasi-linear behaviour of $\chi(f)$ (Figures 4a and c) shows that energy dissipation within the mantle is almost "dry." Such behaviour of mantle η may generally be expected from the dry-friction force σ_D in (6) increasing with pressure (Knopoff & MacDonald, 1958). Within the liquid core, a "fluid-" type dissipation also appears reasonable, which is also supported by the attenuation coefficients of radial modes showing a near-ω^2 frequency dependence (Figure 4a).

Inversion

In the inversion, we focused on the principal structures within the mantle and look for minimal, best-constrained features of the model. Only the shear viscosity parameter η_ε was considered, and eqs. (12) were discretized by using a set of basis functions of radius, *r*. The inner- and outer core and the crust were represented by constant-η_ε layers, and between these layers, $\eta_\varepsilon(r)$ were viewed as a continuous piecewise-linear function of radius (Figure 5a). Because these basis functions $\phi_j(r)$ satisfy $\sum_j \phi_j(r) \equiv 1$ for any *r*, eqs. (12) can be written in matrix form as:

$$\boldsymbol{\chi} = \mathbf{L}\boldsymbol{\eta}_\varepsilon \text{, where: } L_{nj} = \frac{4\pi}{\delta\chi_n \tau_r^2 \langle E_{total} \rangle_n} \int_0^R \left(\dot{\tilde{\varepsilon}}_{ij} \dot{\tilde{\varepsilon}}_{ij} \tau_r^2 \right)^{\nu_\varepsilon} \phi_j(r) r^2 dr \,, \tag{30}$$

R denotes the radius of the Earth, and the integral is evaluated for oscillation mode *n* (here, *n* denotes both the radial and azimuthal mode numbers). Vector $\boldsymbol{\eta}_\varepsilon$ in this equation contains the values of viscosity at the nodal points, between which the viscosity is linearly interpolated. To reduce the risk of numerical underflow, model parameters $\eta_{\varepsilon,j}$ and L_{nj} were re-scaled to ensure $\max_n L_{nj} = 1$ for every *j*. Vector $\boldsymbol{\chi}$ consists of the observed values of χ_n for each mode divided by the corresponding measurement uncertainty, $\delta\chi_n$ (Widmer *et al.*, 1991).

Equation (30) was solved subject to the constraint $\eta_\varepsilon \geq 0$ at all nodes by using an iterative backprojection-type method. Starting from the least-squares inverse, $\boldsymbol{\eta}_\varepsilon = \left(\mathbf{L}^T\mathbf{L}\right)^{-1}\mathbf{L}^T\boldsymbol{\chi}$, we replaced the inverse matrix with its diagonal: $\boldsymbol{\eta}_\varepsilon = \left[diag\left(\mathbf{L}^T\mathbf{L}\right)\right]^{-1}\mathbf{L}^T\boldsymbol{\chi}$, and applied this inverse iteratively:

$$\boldsymbol{\eta}_{\varepsilon}^{i} = \boldsymbol{\eta}_{\varepsilon}^{i-1} + \lambda \left[diag\left(\mathbf{L}^{T}\mathbf{L}\right)\right]^{-1} \mathbf{L}^{T}\left[\boldsymbol{\chi} - \mathbf{L}\boldsymbol{\eta}_{\varepsilon}^{i-1}\right], \tag{31}$$

where i is the iteration number, and parameter $\lambda \approx 0.1$–0.3 is used to "slow down" the approach to the solution. After each iteration, solution (31) was trimmed by replacing negative values of η_{ε} with zeros.

Multiple inversions (31) were performed while testing for the optimal placement of depth nodes (Figure 5a) and exponent ν_{ε} within the depth intervals mentioned above. During the tests, we did not only try minimizing the total squared error for the entire dataset, but sometimes sacrificed it to improve the fit within each of the mode groups (Figure 6, bottom). In particular, radial modes, apparently as the least represented in the data, have the greatest misfits. The resulting model is shown in Figure 5b. The squared normalized data misfit for this model, $e = \sum_{n=1}^{N}\left(\chi_n - \chi_n^{\text{model}}\right)^2 \Big/ N$, equals 6.7, and for the radial, spheroidal fundamental, overtones, and toroidal modes, the misfits are 21.6, 2.2, 7.0, and 6.8, respectively. The data fit is thus poorer than in QM1 ($e \approx 2.0$; Widmer *et al*., 1991) but better than for PREM ($e \approx 17$), and appears reasonable overall (Figure 7), considering our modest goal of making the first step in a completely different physical picture of attenuation.

The key features of the seismic viscosity model (Figure 5b) appear to be robust and supported by the data: 1) very high viscosity of the lithospheric lid and the crust; 2) viscosity generally increasing from the upper to lower mantle, with several (two in the inversion shown here) zones of reduced viscosity, and 3) zero viscosity within the outer core. Broadly, the upper mantle of this model is similar to model QM1 (Figure 5b), although their quantitative comparison appears difficult. As anticipated at the beginning of this article, our model allows some elastic-energy dissipation within the top of the outer core, although the extent and shape of this zone is poorly constrained.

The relative strength of attenuation inverted within the inner core is much lower than in QM1 (Figure 5b). The inner-core η_{ε} is constrained by spheroidal overtones (Figure 8), and it would be useful to estimate whether this η_{ε} would significantly increase if we could fit the overtones more accurately. To estimate this potential increase, we compared the residual data errors to the columns of the forward kernel $\mathbf{L}$ corresponding to the core layers (Figure 8). The root-mean square amplitude of $\mathbf{L}$ for these overtones is $\delta L \approx 0.17$, and estimating the unmodelled error of overtone $\boldsymbol{\chi}$ as approximately $\delta\chi \approx 2.0$ (Figure 8), we obtain the corresponding error of $\boldsymbol{\eta}_{\varepsilon}$ as $\delta\eta_{\varepsilon} \approx \delta\chi/\delta L \approx 12$. A model with the attenuation within the core increased by the amount of this error is shown by thick dashed lines in Figure 5b. As we see, this correction is relatively insignificant, and η_{ε} within the inner core should indeed be at least 5–10 times lower than within the upper mantle.

As our model suggests that the inner-core attenuation is ~10 times lower than in model QM1 (Figure 5b), it appears to be in an even stronger conflict with body-wave dispersion studies. Cormier *et al*. (1998) noted that when corrected for the frequency dependence of Q, the inner-core $Q_{\mu} \approx 110$ in model QM1 gives a P-wave $Q_P^{-1} \approx 0.00128$, which is too low for explaining the interpreted body-wave levels Q_{body}^{-1} from ~0.0025 to 0.005. Cormier and Li (2002) suggested scattering as the likely mechanism of the additional body-wave attenuation within the inner core. However, the above argument is again entirely based on the viscoelastic model. If we are not constrained by this model, the $Q_P^{-1} \propto \omega$ dependence (eq. (25) and Figure 4a) would readily

reconcile the relatively high Q_{body}^{-1} and low attenuation of free oscillations. Frequency dependencies of the inner-core t^* values from PKIKP observations by Doornboos (1983) also show that the $\chi \propto \omega^2$, $Q_P^{-1} \propto \omega$ trend is a good approximation for the inner-core attenuation (Figure 9). Taking $f_{\text{body}} \approx 0.1$ Hz and $f_{\text{free}} \approx 3$ mHz as the characteristic frequencies of these observations and the higher estimate for Q_{body}^{-1} above, the free-oscillation Q_P^{-1} should equal ~10^{-4}, from which $Q_\mu^{-1} \approx 2 \cdot 10^{-4}$. This is ~45 times lower than in model QM1 and ~60 times lower than in PREM. Thus, the anelasticity of the inner core should indeed be weak (Figure 5b). Scattering within the inner core (Cormier and Li, 2002) and near its boundary should further attenuate body waves and decrease the requirement for viscous energy dissipation.

The parameterization selected in our inversion was relatively crude (14 parameters compared to 27 in model QM1; Widmer *et al*., 1991) and selected to generally correspond to the radial periods of the eigenfunctions (Figure 3). Numerous experiments with this parameterization showed that increasing the detail of sampling of the upper mantle reduce the data misfits only slightly while creating models with strong depth variations. Qualitatively, the cause of such variations can be seen from the forward kernels for viscosity (Figure 6). Scaling in these plots is roughly proportional to the 1:6:2:1.3 ratios of the attenuation coefficients of the fundamental spheroidal, radial, spheroidal overtones, and toroidal modes, respectively, at ~4 mHz (Figures 4a and c), so that equal amplitudes in these plots correspond to approximately correct relative attenuations of these modes. Most of the response in the observed attenuation coefficients comes from the range of radii of 5800–6300 km; at the same time, the contributions from this region underestimate the radial-mode χ (compare Figures 6a and b). The inversion therefore tends to place strong bands of attenuation below this depth, and the radial-mode χ ends up somewhat overestimated (Figures 6a, bottom, and 7a). In summary, although the inverse problem is underconstrained and allows significant uncertainties, the data for the different modes are also somewhat inconsistent. Such data conflicts could be resolved by introducing additional detail into the model; however, this should apparently be done with an account for the 3D structure of the upper mantle.

Discussion

The model presented here is far from being complete and only represents an illustration of the change in the picture of Earth's attenuation that arises from replacing the viscoelastic medium Q with mechanical quantities. Many questions need to be answered before a more detailed model can be constructed and compared to the existing Q models in detail. First, our forward kernels (12) differ from the traditional kernels for $q = 1000/Q$, which are inferred from the phase-velocity kernels by using the correspondence principle. As argued before (Morozov, submitted to *Phys. Earth Planet. Inter.*), such phase-velocity kernels overestimate the amount of total dissipated energy, and therefore we can expect an increase in the *in situ* attenuation levels in the new model.

Second, frequency dependencies of the forward kernels are inherently different in the present and the Q-based approaches. In viscoelastic inversions, such as QM1 (Widmer *et al*., 1991), a constant Q is often assumed, which corresponds to energy-dissipation rates proportional to frequency. For free oscillations, this assumption is equally difficult to support or negate, because every normal mode has only a single frequency. In our model, the approach to this problem is conceptually different. Frequency dependence of the energy dissipation rate is not specified (and in fact, undefined at all) but arises from the selected functional form of the dissipation function (11), which is based on fundamental symmetries of the dynamic system in the time-spatial domain. Therefore, in the Q model, the near-linear increase of attenuation with

frequency arises from the postulated constant Q, whereas in our model, this increase follows from the spatial variations of the dissipation kernels with frequency (Figure 6). Interestingly, a Q-type model is easier to fit to the fundamental-mode data, because its built-in frequency dependence mimics the observed near-linear $\chi(f)$ (Figure 7). We tested this by replacing the $\propto \omega^2$ dependence of the dissipation function (10) with ω, which allowed reducing the data error to $e \approx 2.5$ in the inversions. However, this was achieved at the cost of violating the physical principles of the model and making viscosities frequency-dependent (Figure 2b), which does not appear as an acceptable approach.

Interpretation in terms of a rigorous mechanical property (viscosity, *i.e.*, traction per unit of deformation rate) is a major advantage of the proposed model. Both viscosity and elasticity are naturally incorporated in rigorous mechanical formulations such as described above, and the same quantities represent the key attributes of many geodynamic models. By contrast, the *in situ* Q remains a quantity designed specifically for explaining the seismic data, and only within the viscoelastic model. At the heart of this model, there lies the notion of material memory, which "…is hardly satisfying in view the absence of any observations of memory phenomena in the macroscopic behaviour of matter" (Knopoff & MacDonald, 1958). By contrast, the mechanical model above explains energy dissipation and many other phenomena by general physical principles.

As shown above, the absolute values of η_ε are difficult to directly compare to Q, and so let us check whether the trends of their variations may be correlated. Our model (10)–(11) suggests that zones of increased viscosity within the mantle should exhibit a lower Q_μ, *i.e.* plane S waves in them should dissipate faster. However, some authors (Lawrence & Wysession, 2006) used an opposite correlation, which was apparently based on an expectation that a more viscous part of a fluid should deform less when a wave passes through it. However, such decreased deformation means lower amplitudes and still implies a greater relative portion of energy dissipated, in accordance with eq. (10). Therefore, Q should still be reduced within viscous parts of the medium.

A comparison of the seismic viscosity model with several mantle viscosity profiles derived from geodynamic studies reveals some interesting parallels (Figure 10). Compared to PREM and QM1, our model suggests much stronger layering, which is similar to the layering in geodynamic models. This correlation is particularly notable near the surface and within the radial range of ~ 3500–5000 km (Figure 10). This suggests that such layering could indeed be present within the lower mantle. At the same time, the range of η_ε variations across the mantle in seismic models spans about an order of magnitude, whereas geodynamic models show viscosity variations by 2–4 orders of magnitude. The absolute values of seismic η_ε are also 11–12 orders of magnitude lower than those of its geodynamic counterpart. Qualitatively, the latter fact can be understood if we note that the geodynamic viscosity represents the resistance to persistent mantle flows occurring at the time scales of $\sim 10^5$ years, whereas η_ε describes the internal friction in reversible deformations at time scales less than 1 hour. One can say that in geodynamic models, the mantle is treated as a fluid with a near-solid behaviour, whereas in our model (10)–(11), we regard the mantle as an elastic solid with some fluid viscosity. The level of $\eta_M \approx 10^{14}$ Pa·s estimated from laboratory creep above is intermediate between these two values, which also appears reasonable. However, such large range between the values of seismic, lab and geodynamic viscosities deserves further quantitative analysis.

The model presented here is only an initial attempt and poses numerous questions for further studies. In particular, the model needs to be refined to allow constraining the viscosities of the inner and outer cores, which should be done concurrently with accounting for the 3D structure within the mantle. The physical mechanisms of attenuation, and in particular the selections of the

power-law exponents ν in eq. (11) need to be understood and improved. Relations to the attenuation of surface, body, ScS multiples, PKIKP dispersion and other effects used in attenuation studies need to be clarified. The strictly mechanical formulation should provide a basis for creating a unified description of attenuation for all seismic waves. In addition, the new model may have implications not only for the attenuation, but also for the more basic structural and geodynamic models of the Earth. If some energy dissipation occurs within the outer core, this dissipation should change the distribution of stresses within the Earth and consequently modify the normal-mode frequency spectra. Therefore, the internal structure of the Earth may need to be altered as a result of the new physics introduced in this model. Finally, the relations of the new model to the existing 1D and 3D Q-factor inversions are unclear, principally because of he differences in their physical principles and frequency dependencies. These problems are still not addressed in the present solution and will need to be considered in the future.

Conclusions

Observations of elastic-wave attenuation within the Earth can be explained variations of viscosity instead of the commonly used Q_μ and Q_K factors. Interpretation in terms of standard mechanical rather than viscoelastic parameters allows straightforward comparisons between different wave types and physical processes. In particular, the seismic viscosity model can be directly compared to the viscosities used in geodynamic models. All creep phenomena and attenuation of traveling and standing waves are also rigorously described by the viscosity model. The level of viscosity required for explaining the laboratory creep is $\sim 10^{14}$ Pa·s. Comparison to the traditional Q models of the Earth is less straightforward because of the frequency dependencies built into the Q paradigm.

Free-oscillation data by Widmer *et al*. (1991) transformed into the attenuation-coefficient form show near-linear trends of attenuation coefficients with frequency, which suggests a partly "dry" (Coulomb) friction within the mantle. Within the core, the viscosity appears to be of a more "wet" type, which is typical, for example, to saturated porous sedimentary rock. This is supported by observations of the attenuation coefficients proportional to squared frequencies for both radial normal modes and PKIKP body waves.

Inversion of the normal-mode Q dataset suggests pronounced layering of viscosity within the Earth, and particularly within the lower mantle. Seismic viscosity is $\sim 30 \cdot 10^{10}$ Pa·s within the mantle lid, ~ 6–$10 \cdot 10^{10}$ Pa·s within the upper mantle, and 6 to $20 \cdot 10^{10}$ Pa·s within the lower-mantle layers. Within the outer core, the viscosity is undetectably low in the present model, and the inner-core viscosity is ~ 0.5–$1 \cdot 10^{10}$ Pa·s. Thus, by contrast to the existing models, the attenuation within the inner core should be much weaker than within the mantle.

Acknowledgments

This research was supported by NSERC Discovery Grant RGPIN261610-03. The normal-mode dataset by Widmer *et al*. (1991) was used in this study. Normal-mode eigenfunctions were generated by using Mineos package (http://geodynamics.org/cig/software/mineos), GNU Octave software (http://www.gnu.org/software/octave/) was used for inversion, and GMT programs (Wessel & Smith, 1995) were used for preparing illustrations.

References

Aki, K., & Richards, P. G., 2002. Quantitative Seismology, second ed., University Science Books, Sausalito, CA.

Anderson, D. L., & Archambeau, C. B., 1964. The anelasticity of the Earth, *J. Geophys. Res.*, **69**, 2071–2084.

Beskos, D. E., Papadakis C. N., & Woo, H. S. 1989. Dynamics of saturated rocks. III: Rayleigh waves, *J. Engrg. Mech*., **115**, 1017–1034

Bhattacharyya, J., Shearer, P., & Masters, G. 1996. Global lateral variations of shear wave attenuation in the upper mantle, *J. Geophys. Res*., **101**, 22273–22289.

Biot, M. A., 1956. Theory of propagation of elastic waves in a fluid-saturated porous solid, II. Higher-frequency range, *J. Acoust. Soc. Am*., **28**, 168–178.

Bourbié, T., Coussy, O., & Zinsiger, B., 1987. *Acoustics of porous media*, Editions TECHNIP, France, ISBN 2-7108-0516-2

Carcione, J. M., 2007. *Wave fields in real media: Wave propagation in anisotropic anelastic, porous, and electromagnetic media*. Second Edition, Elsevier

Cormier, V. F., 2011. Seismic viscoelastic attenuation, *in*: Gupta, H. K., (ed.), Encyclopedia of Solid Earth Geophysics, doi: 10.1007/978-90-481-8702-7, p.

Cormier, V. F., Li, X., & Choy, G. L., 1998. Seismic attenuation of the inner core: Viscoelastic or stratigraphic?, *Geophys. Res. Lett*., **25**, 4019– 4022.

Cormier V.F, & Li, X., 2002. Frequency-dependent seismic attenuation in the inner core, 2. A scattering and fabric interpretation, *J. Geophys. Res.* **107**, 2362, doi:10.1029/2002JB001796

Dahlen, F.A., & Tromp, J, 1998. *Theoretical global seismology*, Princeton Univ. Press, Princeton, NJ, 1025 pp.

Gilbert, F. & Dziewonski, A. M., 1975. An application of normal mode theory to the retrieval of structural parameters and source mechanisms from seismic spectra, *Phil. Trans. R. Soc. Lond*., A **278**, 187–269.

Deresiewicz, H., 1960. The effect of boundaries on wave propagation in a liquid-filled porous solid: I. Reflection of plane waves at a free plane boundary (non-dissipative case). *Bull. Seismol. Soc. Am.,* **50**, 599–607.

Doornbos, D.J., 1983. Observable effects of the seismic absorption band in the Earth, *Geophys. J. R. Astr*. *Soc.* **75**, 693–711

Durek, J., & Ekström, G., 1996. A radial model of anelasticity consistent with long-period surface-wave attenuation. *Bull. Seismol. Soc. Am*., **86**, 144–158.

Durek, J., & Ekström, G., 1997. Investigating discrepancies among measurements of traveling and standing wave attenuation. *J. Geophys. Res*., **102**, 24529–24544.

Dziewonski, A. M., & Anderson, D. L. (1981), Preliminary Reference Earth Model (PREM), *Phys. Earth Planet. Inter*., **25**, 297–356

Forte, A. M., & Mitrovica, J. X., 1996. New inferences of mantle viscosity from joint inversion of long-wavelength mantle convection and post-glacial rebound data, *Geophys. Res. Lett*., **23**, 1147–1150.

Forte, A. M., & Mitrovica, J. X., 2001. Deep-mantle high-viscosity flow and thermochemical structure inferred from seismic and geodynamic data, *Nature*, **410**, 1049–1056.

Hager, B.H., & Richards, M. A. (1989). Long-wavelength variations in Earth's geoid: physical models and dynamical implications, *Philos. Trans. R. Soc. Lond*. **A328**, 309–327.

Kanamori, H., & Anderson, D. L., 1977. Importance of physical dispersion in surface wave and free oscillation problems: review, *Rev. Geoph. Space Phys*. **15**, 105–112

Knopoff, L., & MacDonald, G. J. F., 1958. Attenuation of small amplitude stress waves in solids, *Rev. Mod. Phys*., **30**, 1178–1192

Landau, L. D., & Lifshitz, E. M., 1976. *Mechanics*, Course of theoretical physics, volume 1 (3rd edition), Elsevier, ISBN 978-0-7506-2896-9.

Landau, L. D., & Lifshitz, E. M., 1987. *Fluid mechanics*, Course of theoretical physics, volume 6 (2nd revised

edition), Elsevier, ISBN 978-0-7506-2767-2

Laske, G. & Widmer-Schnidrig, R., 2009. Theory and Observations – Normal-mode and surface wave measurements, *in*: Romanowicz, B., and Dziewonski, A. (Eds.) Treatise on Geophysics, v. 1, Seismology and Structure of the Earth, ISBN 978-0-444-53459-0, 67–125.

Lawrence, J. F., & Wysession, M. E., 2006. QLM9: A new radial quality factor (Q_μ) model for the lower mantle, *Earth Planet. Sci. Lett*., **241**, 962–971.

Lekić, V., Matas, J., Panning, M., & Romanowicz, B., 2009. Measurement and implications of frequency dependence of attenuation. *Earth and Planet. Sci. Lett*., 282, 285-293.

Lomnitz, C., 1956. Creep measurements in igneous rocks, *J. Geology*, 64, 473–479.

Li, X., & Cormier, V.F., 2002. Frequency-dependent seismic attenuation in the inner core, 1. A viscoelastic interpretation, *J. Geophys. Res.*, **107**, 2361, doi:10.1029/2002JB001795.

McNamara, A.K., van Keken, P. E., & Karato, S.-I., 2003. Development of finite strain in the convecting lower mantle and its implications to seismic anisotropy, *J. Geophys. Res*. **108**(B5), 2230, doi:10.1029/2002JB001970.

Morozov, I. B., 2008a. Open-source software integrates data analysis, *EOS Trans. Am. Geophys., U*. **89** (29), 261-262.

Morozov, I. B., 2008b. Geometrical attenuation, frequency dependence of *Q*, and the absorption band problem, *Geophys. J. Int*., **175**, 239–252.

Morozov, I. B., 2009. On the use of quality factor in seismology. AGU Fall Meeting, San Francisco, CA, Dec 14–18, 2009, S44A-02.

Morozov, I. B., 2010a. On the causes of frequency-dependent apparent seismological *Q*. *Pure Appl. Geophys*., **167**, 1131–1146, doi 10.1007/s00024-010-0100-6

Morozov, I. B., 2010b. Attenuation coefficients of Rayleigh and *Lg* waves, *J. Seismol*. **14**, 803–822, doi: 10.1007/s10950-010-9196-5

Morozov, I. B. 2010c. Attenuation without *Q*, Trafford, ISBN 978-1-4269-4525-0, 354 pp.

Morozov I. B., 2011. Anelastic acoustic impedance and the correspondence principle. *Geophys. Prosp*., **59**, 24–34, doi 10.1111/j.1365-2478.2010.00890.x

Morozov I. B., Modeling and inversion of Love-wave attenuation, submitted to *Phys. Earth. Planet. Inter.*

Morozov, I. B., & Pavlis, G. L., 2011. Management of large seismic datasets: I. Automated building and updating using BREQ_FAST and NetDC, *Seismol. Res. Lett.*, **82** (2)

Romanowicz, B. & Mitchell, B. J., 2009. Deep Earth structure – *Q* of the Earth from crust to core, *in*: Romanowicz, B., & Dziewonski, A. (Eds.) Treatise on Geophysics, v. 1, Seismology and Structure of the Earth, ISBN 978-0-444-53459-0, p. 731–774.

Wessel, P., & Smith, W. H. F., 1995. New version of the Generic Mapping Tools released, *EOS, Trans. Am. Geophys. Union*, **76**, 329.

Widmer, R., Masters, G., & Gilbert, F., 1991. Spherically symmetric attenuation within the Earth from normal mode data, *Geophys. J. Int*., **104**, 541–553.

Woodhouse, J. H., & Deuss, A., 2009. Theory and observations – Earth's free oscillations, *in*: Romanowicz, B., & Dziewonski, A. (Eds.) Treatise on Geophysics, v. 1, Seismology and Structure of the Earth, ISBN 978-0-444-53459-0, p. 31–65.

Figures

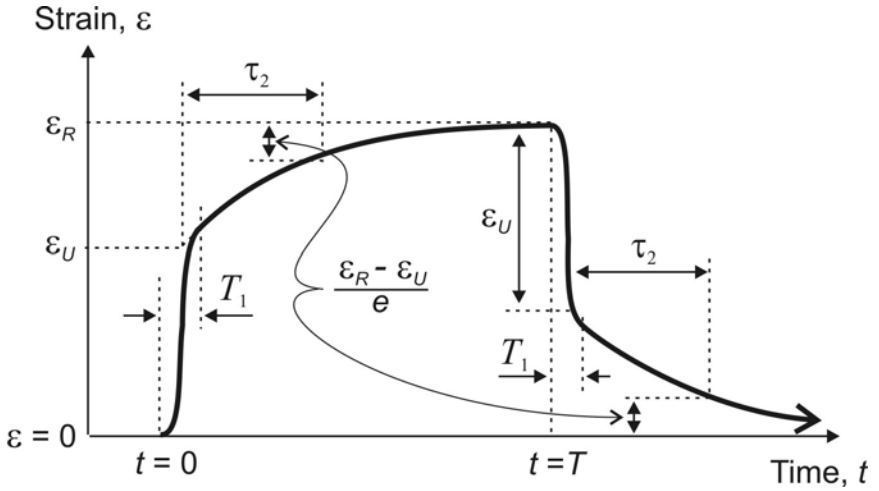

Figure 1. Quasi-static creep model in eqs. (16)–(21). Constant stress is applied at time $t = 0$ and released at $t = T$. After a rapid equilibration over time intervals T_1, the stress becomes partly compensated by viscous forces leading to initial (unrelaxed) strain ε_U. The relaxation time is denoted τ_2. At $t >> \tau_2$, the strain increases to relaxed value of ε_R, and viscous forces disappear.

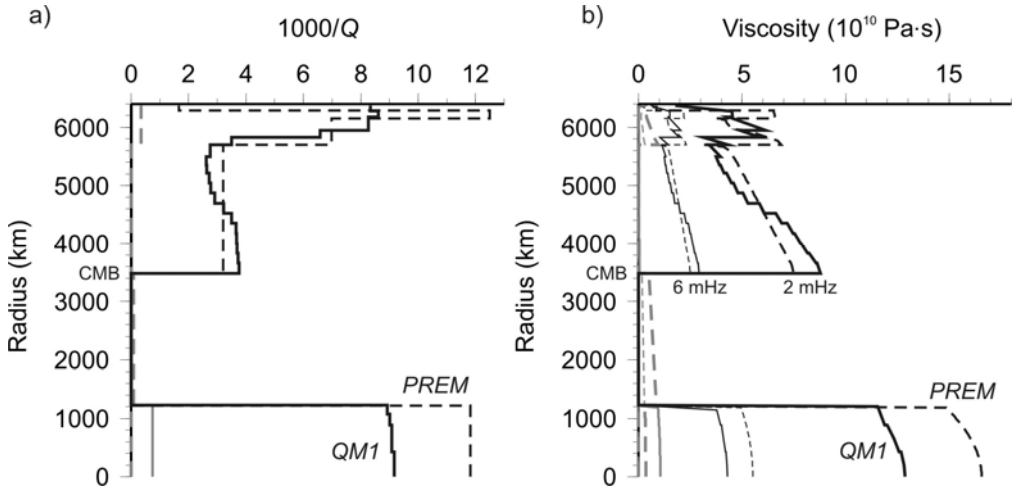

Figure 2. Global models of seismic anelasticity QM1 (Widmer *et al*., 1991; solid lines) and PREM (Dziewonski & Anderson, 1981; dashed lines): a) in $q = 1000/Q$ form; b) transformed to viscosities η_μ and η_Δ by using eqs. (25) and (31). Black lines correspond to shear attenuation (q_μ and η_μ), and grey lines show the bulk attenuation (q_K and η_Δ, respectively). In plot b), the conversion is shown for frequencies of 2 mHz (thick lines) and 6 mHz (thin lines). Label CMB indicates the core-mantle boundary.

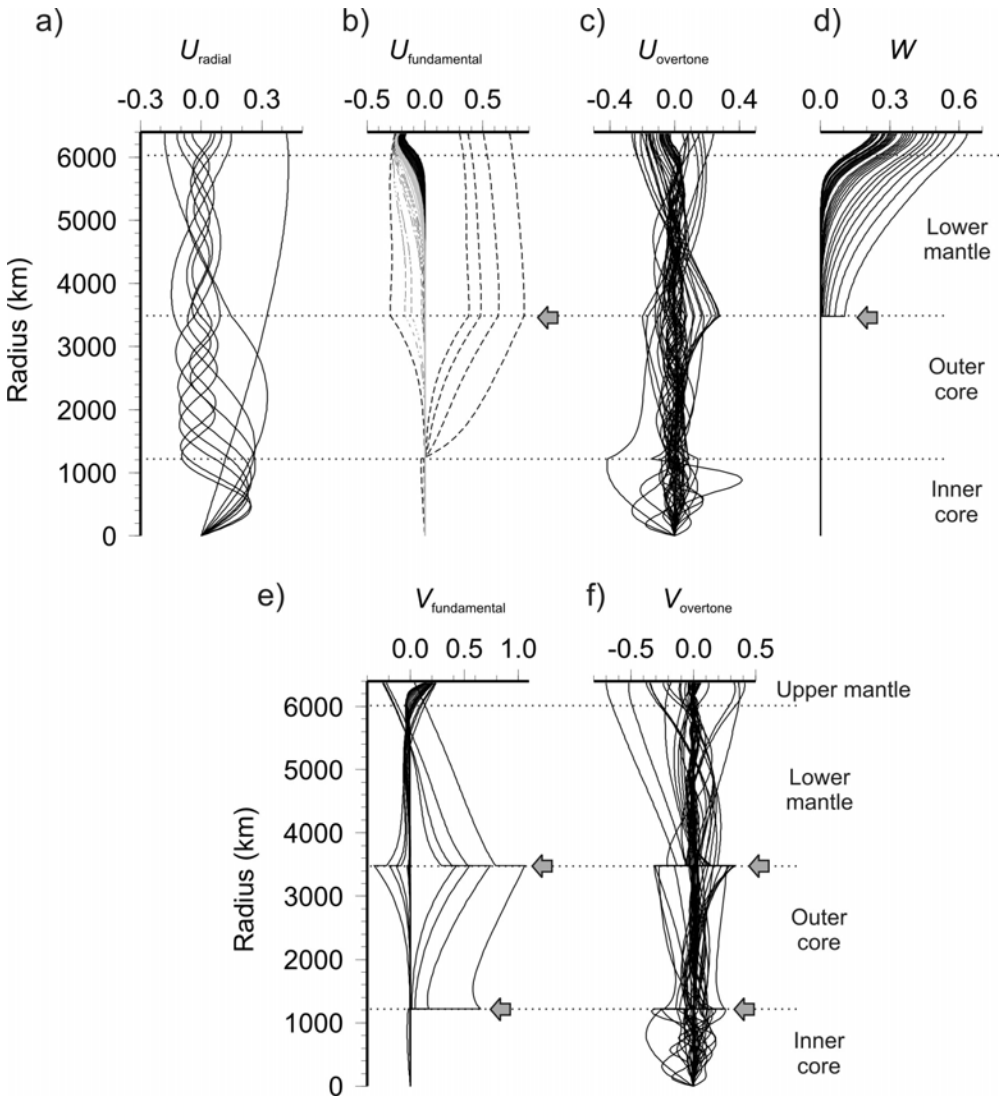

Figure 3. Normal modes in elastic PREM model: a) radial, b) and e) fundamental spheroidal, c) and f) spheroidal overtones, and d) fundamental toroidal. In plot b), dashed lines indicate the U scalar for modes with frequencies $f_0 < 2.5$ mHz, grey lines correspond to 2.5 mHz $< f_0 <$ 3.5 mHz, and modes with $f_0 > 3.5$ mHz are shown in black. Grey arrows indicate areas of strong shear strains not accounted for in viscoelastic inversions.

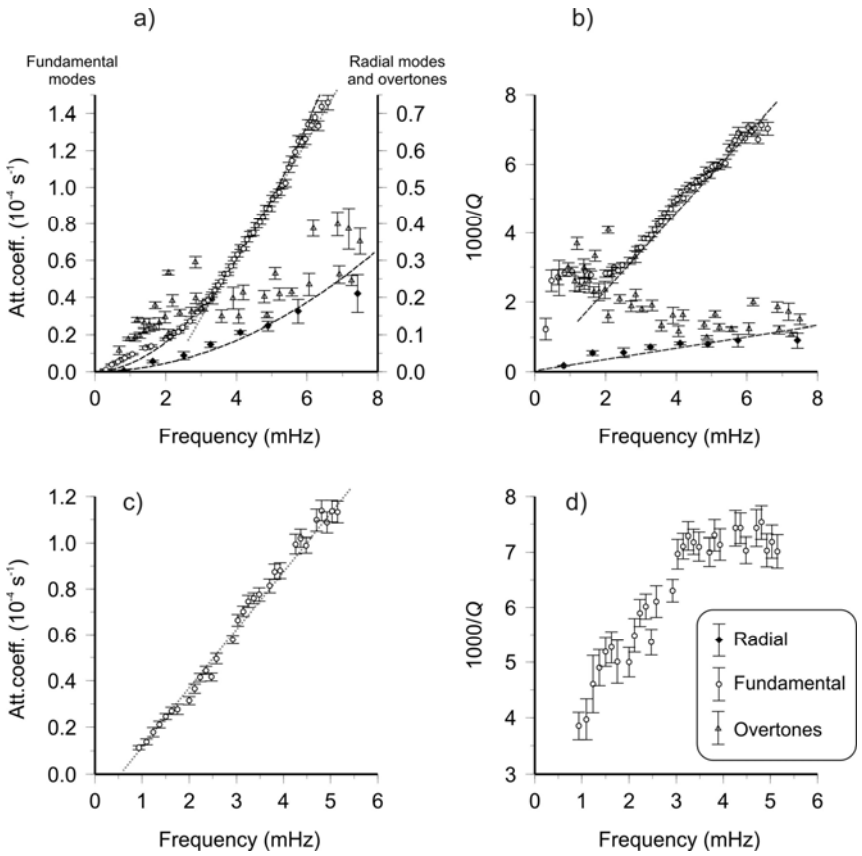

Figure 4. Normal-mode attenuation used in this study (Widmer *et al*., 1991): a) χ for spheroidal modes, b) the same data in the form of $q = 1000/Q$, c) and d) similar plots for toroidal modes. Radial, fundamental, and toroidal-mode data are shown by different symbols (legend). In plot a), note the difference in scales for the fundamental and other modes. Dashed lines in plots a) and b) indicate the $\chi \propto \omega^2$, $q \propto \omega$ trends for radial and higher-frequency fundamental modes suggested in the text. Grey dotted lines in plots a) and c) show empirical linear trends in $\chi(f)$.

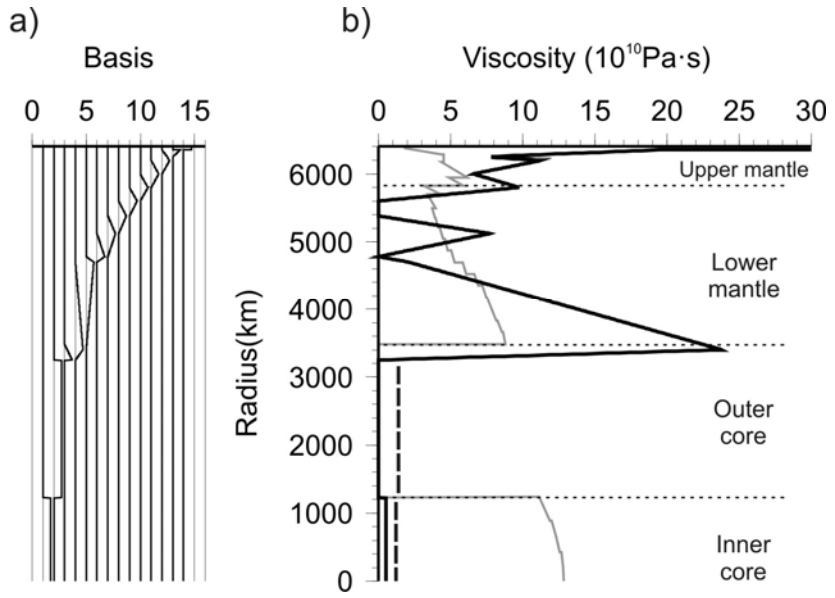

Figure 5. Inversion for η_ε: 1) piecewise-linear basis functions, b) resulting model. For comparison, model QM1 converted to η_ε at 2 mHz (Figure 2b) is also shown (grey). Thick dashed lines indicate the estimated upper bounds on η_ε within the core estimated from the residual errors of the attenuation coefficients fro spheroidal overtones.

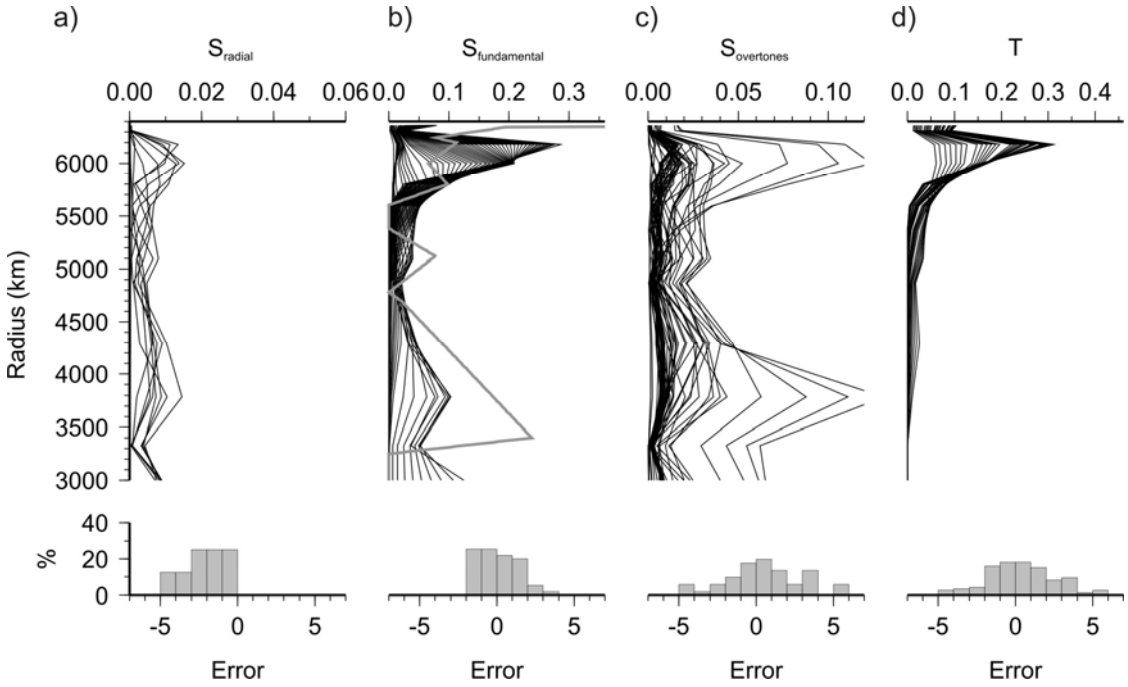

Figure 6. Depth distributions of η_ε kernels for different groups of modes: a) radial, b) fundamental spheroidal, c) spheroidal overtones, and d) fundamental toroidal. Bottom plots show histograms of the corresponding data misfits resulting from model in Figure 5b.

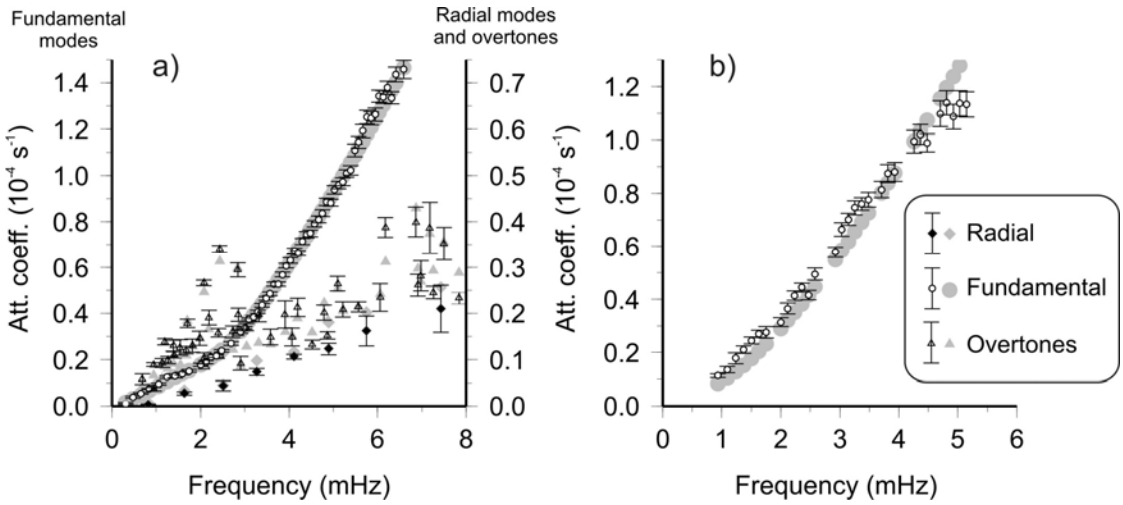

Figure 7. Data fit in the final model (Figure 5b): a) spheroidal modes, b) toroidal modes. Symbols indicate the measured attenuation coefficients as in Figures 4a and c, grey symbols are the corresponding modelled values.

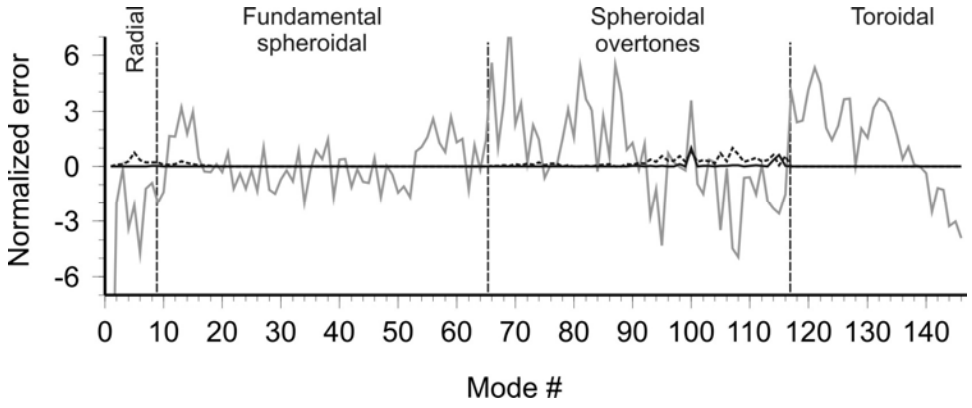

Figure 8. Normalized data errors in the final model (grey line). Mode groups are indicated. Black lines are the columns of the forward kernel **L** for the inner core (solid) and outer core (dashed).

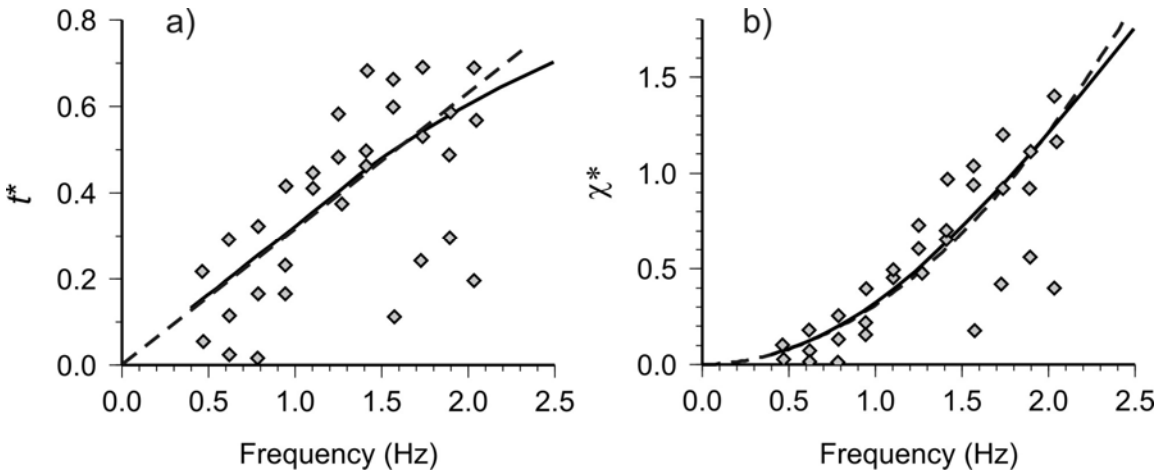

Figure 9. Inner-core attenuation data from *PKIKP* to PKP_{BC} spectral ratios between 147° and 151° source-receiver ranges by Doornbos (1983): a) the original t^* data; b) the same data in the attenuation-coefficient form $\chi^* = \pi f t^*$. Solid lines indicate the trend interpreted by Doornbos (1983), dashed lines show the quadratic trend $\chi^* \propto \omega^2$, which is equivalent to t^* and $Q^{-1} \propto \omega$.

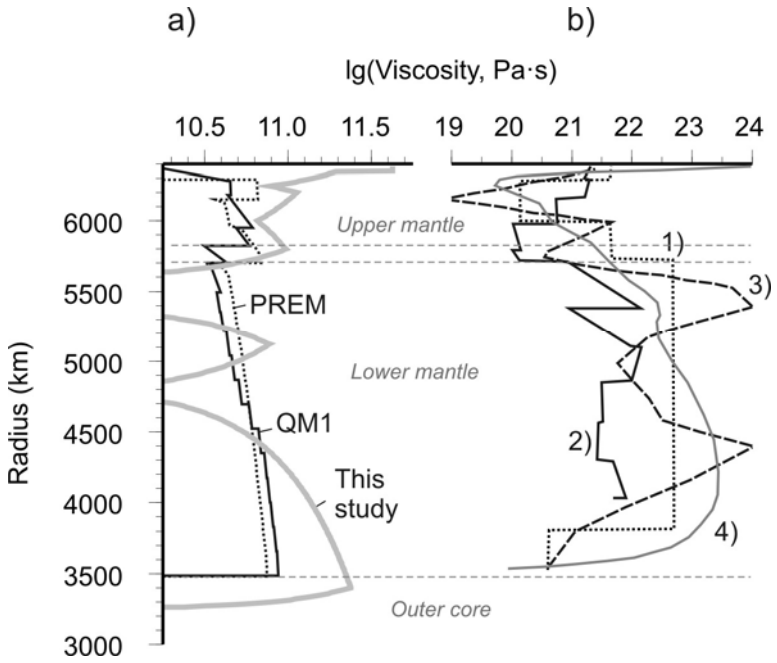

Figure 10. Mantle viscosities: a) from inversions of free-oscillation seismic data (labelled); b) from geodynamic studies: 1) Hager & Richards (1989), 2) Forte & Mitrovica (2001), 3) Forte & Mitrovica (1996), and 4) McNamara *et al*. (2003).